Estimating Chlorophyll Content in a Mangrove Forest Using a Neighbourhood Based Inversion Approach

Giles Jay Williams
February 2012

Course Title: Geo-Information Science and Earth Observation for Environmental Modelling and Management

Level: Master of Science (MSc)

Course Duration: August 2010 – March 2012

Consortium Partners: Lund University (Sweden)
University of Twente, Faculty ITC (The Netherlands)

Estimating Chlorophyll Content In A Mangrove Forest Using A Neighbourhood Based Inversion Approach

by

Giles Jay Williams

Thesis submitted to the Faculty of Geo-Information Science and Earth Observation, University of Twente in partial fulfilment of the requirements for the degree of Master of Science in Geo-information Science and Earth Observation for Environmental Modelling and Management

Thesis Assessment Board

Dr. Ir. C.A.M.J. de Bie (Chair)
Dr. M.F. Noomen (External Examiner)
Prof. Dr. Ing. W. Verhoef (First Supervisor)
Prof. Dr. A.K. Skidmore (Second Supervisor)

UNIVERSITY OF TWENTE.

ITC FACULTY OF GEO-INFORMATION SCIENCE AND EARTH OBSERVATION

Disclaimer

This document describes work undertaken as part of a programme of study at the Faculty of Geo-Information Science and Earth Observation, University of Twente. All views and opinions expressed therein remain the sole responsibility of the author, and do not necessarily represent those of the institute.

Abstract

Mangroves are coastal vegetation that inhabit tropical and sub-tropical regions. High rates of deforestation in mangrove forests are a result of conversion to aquaculture, agriculture and logging. Aquaculture and agriculture result in the release of nutrient rich effluent into the mangrove ecosystem. Effluent is known to contain increased levels of nitrogen and the impact on the mangrove ecosystem is not fully understood. Chlorophyll can be used as an indicator of vegetation health through a high correlation with nitrogen. Inversion of a canopy reflectance model has been previously applied to estimate chlorophyll in mangroves of the Mahakam Delta, East Kalimantan; achieving low accuracy results. The approach is inherently hampered by the ill-posed nature of the solution which results from counterbalancing effects between parameters. In this study, a neighbourhood based inversion developed by Atzberger (2004) was applied to improve the accuracy of chlorophyll estimation. This approach has not been applied previously to tropical or mangrove forests. Inversion was performed using a look up table approach with the Soil Leaf Canopy (SLC) reflectance model.

The neighbourhood inversion approach was not able to significantly improve the accuracy of chlorophyll estimation. Due to the low accuracy, no correlation could be identified between neighbourhood size and accuracy. Compared to the pixel based approach (Rel. RMSE = 31.5% and R^2 = 28.9%), the best results achieved by the neighbourhood inversion were from 3x3 sliding windows (Rel. RMSE = 30.99% and R^2 = 30.38%) and objects with scale factor 5 (Rel. RMSE = 30.61% and R^2 = 30.19%).

A number of errors were identified throughout the data analysis, with the field samples determined to be the most significant source of uncertainty. These uncertainties indicate that the field samples are not sufficiently representative of the image pixels. Although accuracy estimates are low, the output maps from the different methods show a consistent spatial structure. Maps should not be used to estimate chlorophyll at specific locations but can be used to examine spatial variations throughout the study area. Chlorophyll concentration appears to be correlated with proximity to ponds and position relative to the coast.

Acknowledgements

I would like to thank my supervisors Dr. Wouter Verhoef and Dr. Andrew Skidmore for their advice and critical comments.

I would also like to thank Dr. Martin Schlerf for his advice at the start of this thesis and Dr. Michael Weir for his assistance in accessing faster computers.

I am grateful to Alan Rex for his critical comments and helpful discussions especially with data related issues. Special thanks to my GEM colleagues for their continued support and encouragement throughout the past 18 months.

Finally, I would like thank my family, friends and Leah for their support.

Table of Contents

Abstract v
Acknowledgements vi
List of figures viii
List of tables ix
1. Introduction 1
1.1 Mangroves and Shrimp Ponds 1
1.2 Modelling and Inversion 2
1.3 Research Problem 5
1.4 Objectives 6
1.4.1 General Objective 6
1.4.2 Specific Objectives 6
1.4.3 Research Questions 6
2. Materials and Methods 7
2.1 Study Area 7
2.2 Image Data 7
2.3 Field Data and Processing 9
2.4 Chlorophyll Estimation 11
2.4.1 Modelling 11
2.4.2 Pixel-based Inversion 14
2.4.3 Parameter Variation 14
2.4.4 Object Creation 15
2.4.5 Neighbourhood Inversion 15
2.4.6 Validation and Map Generation 17
3. Results 19
3.1 Field Data Calibration 19
3.2 Pixel Based Estimation 19
3.3 Parameter Variation and Object Comparison 20
3.4 Neighbourhood Based Estimation 23
3.5 Chlorophyll Maps 26
4. Discussion 29
5. Conclusion 35
5.1 Recommendations 36
References 37
Appendix 41

List of figures

Figure 1: Conceptual diagram of the mangrove ecosystem.. 5
Figure 2: Map showing the location of the Mahakam delta 8
Figure 3: False colour infra-red image showing forest areas 10
Figure 4: Visual representation simulated spectra stored in the LUT. 12
Figure 5: Soil reflectance sprectrum... 12
Figure 6: Flowchart of the neighbourhood inversion method 16
Figure 7: SPAD to chlorophyll calibration formulae 19
Figure 8: Measured and predicted values using the pixel-based inversion. 20
Figure 9: Simulated and measured spectra using the pixel based method. 21
Figure 10: Parameter variation measured from image data.............................. 22
Figure 11: Comparison between objects created by eCognition and Imagine Objective. 22
Figure 12: Measured and predicted values using a 3x3 window inversion. 23
Figure 13: Measured and predicted chlorophyll using an object inversion. 24
Figure 14: Simulated and measured spectra using the window inversion 25
Figure 15:Semi-variogram of chlorophyll field samples.................................. 26
Figure 16: Map of chlorophyll from the pixel based inversion 27
Figure 17: Map of chlorophyll using the object based inversion. 28
Figure 18: Reflectance per pixel within window neighbourhoods. 41
Figure 19: Reflectance per pixel within object neighbourhoods. 42
Figure 20: False colour mosaic of the Mahakam study area. 43

List of tables

Table 1: Input parameters used for generation of the LUT 13
Table 2: Results of changing window size with a window-based inversion. 24
Table 3: Results of different scale factors using an object-based inversion. 24
Table 4: Summary of errors in the data analysis. 30

1. Introduction

1.1 Mangroves and Shrimp Ponds

Mangroves are salt-tolerant, evergreen, coastal vegetation that inhabit tropical and sub-tropical regions. They are abundant in brackish, inter-tidal areas with low wave and tidal action (Hogarth, 2007). The coastal environment is nutrient deficient and mangroves are highly adapted to these conditions. Mangroves favour areas such as river deltas, where fresh river water mixes with the tidal inundation of sea water to promote nutrient availability and recycling. Mangroves act as a filter, trapping and absorbing nutrients and heavy metals available in the soil (FAO, 2007). They also support a number of ecological functions; providing habitats and spawning grounds for reptiles, amphibians, mammals, birds and fish (Nagelkerken et al., 2008). Local communities exploit mangroves for economic purposes such as fuel wood, construction material and food (FAO, 2007).

High pressure by humans on coastal ecosystems has resulted in high rates of mangrove deforestation globally. The Asian region has been one of the most severely affected. Mangroves in Asia account for 38% of the global total, covering over 5.8 million hectares and approximately 25% of this area was removed during the period 1980-2005. The leading causes for mangrove removal in this region are: conversion to aquaculture for shrimp farming, excessive logging and conversion to agriculture (FAO, 2007).

Shrimp farming results in the release of nutrient rich water into the surrounding areas. Effluents consist of uneaten feed and waste matter which contains increased levels of ammonia, nitrates and phosphates (Ruenglertpanyakul et al., 2004). The effect of shrimp pond effluents on the mangrove ecosystem is not fully understood (Sidik, 2009). However, prolonged high nutrient availability can result in negative changes to mangrove growth (Reef et al., 2010). Consequently, studies are required to examine the impact of aquaculture practices on mangroves. These are essential to the monitoring and protection of mangroves and the sustainable management of the shrimp farming industry. Figure 1 shows a conceptual diagram of the mangrove ecosystem and illustrates components which may be affected by environmental changes.

Foliar biochemicals can be used as indicators of nutrient availability, ecosystem functioning and plant stress (Siciliano et al., 2008; Zarco-Tejada & Sepulcre-Canto, 2007). Nitrogen is one nutrient which limits growth in mangroves (Tomlinson, 1994) and is an effluent from shrimp ponds (J.-L. Martin, 2011; Ruenglertpanyakul et al., 2004). Detection of nitrogen by remote sensing techniques is possible through correlation of field measured concentrations with specific wavelengths and known spectral absorption features. Extensive field sampling is required to build a site specific model. A generalised approach can be applied using data from other sites, but this produces results with lower accuracy (M. E. Martin et al., 2008; Peterson et al., 1988). Foliar nitrogen content can also be estimated through a relationship with chlorophyll (Haboudane et al., 2002; Tilling et al., 2007). Variations in concentration can be used to show differences between healthy and stressed vegetation; chlorophyll concentration decreases when vegetation is stressed (Zarco-Tejada & Sepulcre-Canto, 2007). Estimating variations in mangrove health will be a significant step towards assessing the impact of increased nutrient levels on mangrove vegetation.

1.2 Modelling and Inversion

Hyperspectral imagery is an evolving resource which has been used to improve the efficiency of vegetation monitoring. In other words, the detection of reflected radiation at a finer scale allows a greater amount of information to be extracted from a single dataset (Held et al., 2003) and quantitative estimates of biophysical properties to be retrieved (Ustin et al., 2004). Leaf chlorophyll is most active near the 550nm and 700nm parts of the spectrum (Carter & Spiering, 2002) and the use of hyperspectral data allows these specific parts of the spectrum to be used in analysis. Hyperspectral imagery has been successfully applied to examine vegetation health and ecosystem properties in mixed temperate forests (Huber et al., 2008), needle-leaved evergreen forests (Schlerf et al., 2010) and grasslands (Darvishzadeh et al., 2008).

To obtain quantitative estimates of canopy biochemicals from hyperspectral imagery, two approaches have been developed. Empirical approaches use ratios between narrow spectral bands to create vegetation indices which are correlated to measured vegetation characteristics. The resulting models are site, species and sensor specific and therefore require calibration before use (Zhang et al., 2008). Physically-based approaches use radiative transfer models. Radiative transfer models simulate the interactions of incoming solar radiation with the atmosphere and earth's surface. Vegetation models can simulate the top-of-canopy reflectance using formal knowledge of the biophysical and biochemical characteristics of the canopy and leaves. Using hyperspectral imagery of the canopy, the model can be inverted to provide a quantitative estimate of the vegetation parameters. Model parameterisation is also required, to define parameter ranges applicable to the study area (Goel & Thompson, 2000).

A number of physical models exist for modelling canopy reflectance. Model type and complexity are varied and the model chosen is dependent on the study area, especially the canopy architecture (Goel & Thompson, 2000). Turbid-medium models assume that the canopy is a horizontal, uniform entity with distinct parallel layers. Each layer consists of randomly distributed vegetation elements with absorbing and scattering properties. Turbid-medium models are suitable for dense, horizontally uniform canopies (Goodenough et al., 2006). Geometric models consider a flat ground surface containing geometrical objects to represent tree crowns, in a regular or random distribution. Reflectance is then modelled as a combination of sunlit and shadowed crowns and sunlit and shadowed ground surface. These models are suitable for sparse canopies (Li & Strahler, 1986). Hybrid models combine modelling approaches. In the case of geometric and turbid-medium models, the canopy is modelled as a distribution of geometrical objects containing turbid media with randomly distributed vegetation elements. Additional components such as a soil model may also be included. Hybrid models can be used to represent a wider variety of canopy types (Goel & Thompson, 2000).

Inversion to retrieve vegetation parameters is typically carried out by pixel-based application of the inversion process. Parameter estimates are obtained independently for each pixel in the image by comparing the measured spectrum with a predicted spectrum generated by a canopy reflectance model. Several inversion approaches are available; of which the most commonly applied are numerical optimisation techniques, look-up tables (LUT) and artificial neural networks (ANN). While the 3 approaches can produce highly correlated results (Vohland et al., 2010), advantages and limitations exist for each method. LUT and ANN are considered more computationally efficient than numerical optimisation. However, to ensure suitable representation of the study area in the LUT and ANN training set, a large database of simulated spectra is required. The size of the database required also increases with model complexity. The computation time required for a LUT search increases with increasing database size (Goel & Thompson, 2000; Liang, 2005).

There exists, however, an inherent problem with the inversion method. The inversion solution is considered ill-posed if either no unique solution exists or if the model or measurements contain errors that may result in variation of the solution (Combal et al., 2003). Counterbalancing effects between parameters, results in multiple combinations that can produce almost identical reflectance spectra. Also, radiative transfer models contain simplifications of reality which do not fully represent the actual interaction between the vegetation and incoming radiation (Atzberger, 2004). To counteract the ill-posed nature of model inversion, two different approaches exist. Combal et al. (2003) proposed the use of prior information to reduce uncertainty in parameter estimation. Prior information is used to impose constraints on the parameter space and reduce the number of possible solutions. The prior information can be either: supplementary data from another sensor, knowledge of the canopy architecture or knowledge of the distribution of canopy variables. The approach proposed by Atzberger (2004), is to use a spatially constraint model inversion. This method takes into account the principle of spatial autocorrelation and assumes that canopy variables are similar within neighbouring pixels. Radiometric information from neighbouring pixels is used to create a neighbourhood signature containing spectral covariance information. This is combined with the reflectance data from the pixel of interest to perform the inversion.

Both methods have been evaluated and proved to provide an adequate solution to the ill-posed problem. Advantages and disadvantages exist for both approaches. Application of prior information (Combal et al., 2003) incurs additional costs to carry out fieldwork or obtain supplementary data from other sensors. The neighbourhood based method (Atzberger, 2004; Atzberger & Richter, 2009) utilises a single dataset but requires more complex and rigorous computations. Few previous studies have implemented the neighbourhood approach. These studies focused on structural parameters such as leaf area index (LAI) and only one attempted to estimate foliar chlorophyll. Study areas used in each of the previous works were varied and included simulated data sets and agricultural areas (Atzberger, 2004; Atzberger & Richter, 2009). As these approaches use a physical model for vegetation reflectance, it is expected that estimation of any of the model's parameters can be made. The main limitation being the collection of field samples required for validation of the results.

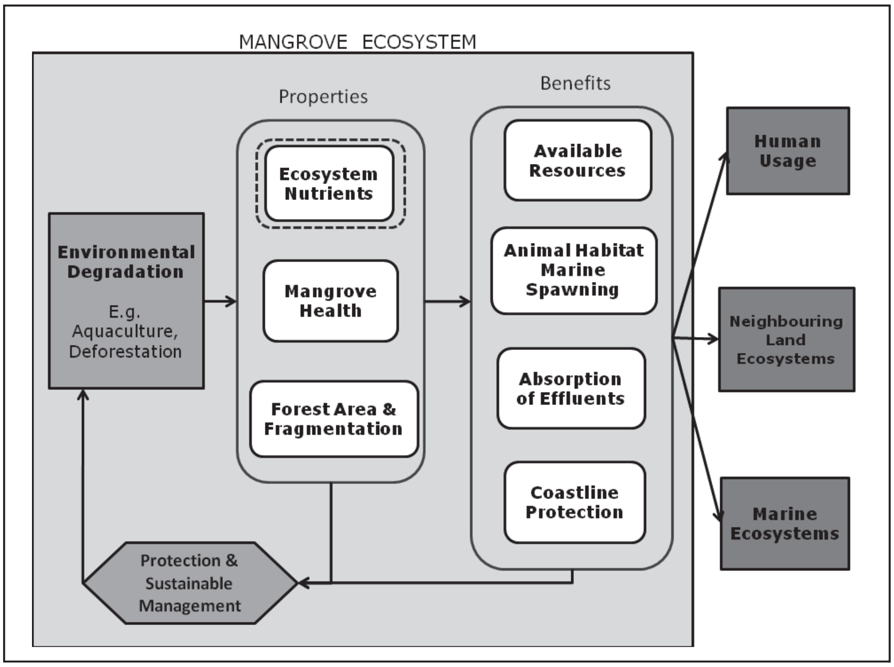

Figure 1: Conceptual diagram of the mangrove ecosystem. The outlined box highlights the component that was targeted in this study.

1.3 Research Problem

A physically based approach has been applied previously to study chlorophyll in mangrove forests. The Soil-Leaf-Canopy (SLC) radiative transfer model was applied to HyMap hyperspectral imagery and inverted in a pixel based approach to retrieve estimates for chlorophyll concentrations in mangrove forests of the Mahakam Delta, Indonesia (Wandera, 2011). The study achieved results of: R^2=0.30 and relative RMSE = 27.5%, when comparing estimated and field measured chlorophyll content.

The study has shown that the traditional inversion approach can provide only fair results when applied to a mangrove canopy. However, as research has shown, this approach is inherently hampered by the ill-posed nature of the inverse problem; which can lead to inaccurate and unstable inversion results (Atzberger, 2004). Further studies are therefore required to apply and test the methods which have been proposed to improve the reliability and accuracy of these results. The neighbourhood based inversion has not been previously applied to a forest or mangrove environment.

1.4 Objectives

1.4.1 General Objective

The objective of this study is to apply a neighbourhood based inversion approach to hyperspectral imagery for estimating chlorophyll content in a mangrove canopy.

1.4.2 Specific Objectives

- To apply the sliding window and image segmentation approaches for neighbourhood based model inversion.
- Evaluate the results against field samples of leaf chlorophyll content
- To compare the accuracy that can be achieved using a neighbourhood based approach with the results of a traditional, pixel based inversion.

1.4.3 Research Questions

- How do mangrove vegetation parameters vary within image neighbourhoods?
- How does the accuracy of parameter retrieval change in relation to neighbourhood size?
- Are the results sufficiently reliable to be used for an assessment of the spatial variations of chlorophyll in mangroves?

2. Materials and Methods

2.1 Study Area

The Mahakam delta is located in the province of East Kalimantan, Indonesia (Figure 2). The fan-shaped delta is made up of 46 islands which are characterised by high biodiversity with at least 7 families and 20 species of mangrove. The central part of the delta once formed one of the largest expanses of *Nypa* mangrove in the world (Sidik, 2009). Ecological functioning of the delta is physically driven by 2 main influences. The 770 km. long Mahakam River discharges fresh water which contains a large volume of nutrient rich sediments. River discharge interacts with the tidal influx of seawater to provide the physical and chemical conditions for mangrove and marine life (Dutrieux, 1991).

The Mahakam delta, Indonesia, is characterised by extensive pond construction for aquaculture. By 2007, 55% of the mangrove area in 1980 was removed. In 2007, the size of the Mahakam delta was estimated at 107,222 ha using Quickbird imagery. 10,645 ponds were recorded, covering 54% (57,912 ha) of the total area. Approximately 80% of the removed mangroves were *Nypa* stands. The most significant impact of the mangrove removal is the gradual increase in saltwater intrusion upstream. This results in changes to the environmental conditions within the delta, mainly increased exposure to higher salinity levels (Sidik, 2009).

The study area was appropriate because it represents common issues associated with mangrove ecosystems globally. The highly biodiverse area is threatened by rapid ecosystem change. Areas like the Mahakam delta can provide insight to how the mangroves are able to adapt to these changes.

2.2 Image Data

Airborne hyperspectal imagery was collected on 16 October 2009 with a HyMap sensor. The data contained 126 spectral bands, covering the range 450nm – 2490nm. 8 flight lines were flown over an area in the north-east of the delta, covering approximately 13.3 km (E-W) by 11.4 km (N-S), with a spatial resolution of 3.1 meters. Imagery was processed by HyVista Corporation, Sydney, Australia. Radiometric corrections were performed using Hycorr software to convert the data to top-of-canopy reflectance. Image geocorrection was also applied HyVista Corporation. Checks were performed on the imagery to assess the data quality after radiometric and geometric corrections had been applied. Ground control points were measured at discernible features in the image using handheld GPS. Coordinates were then compared to those provided by the corrected image. The RMSE accuracy of the georeferenced image was calculated as approximately 6 – 9 meters (2-3 pixels) (Wandera, 2011).

Figure 2: Map showing the location of the Mahakam delta, East Kalimantan, Indonesia. Inset shows an ASAR image of the delta, 2009. (Source: www.eosnap.com, retrieved 1-2-2012)

Co-located pixels from adjacent flight strips were compared to examine the radiometric consistency between different observations of the same ground location. For a single pixel, the maximum difference in a single band was approximately 4% of mean reflectance. A mosaicked image was therefore used instead of individual flight strips. The image was masked to remove areas obscured by clouds and cloud shadows. Forested areas were also masked to remove water bodies, shrimp ponds and other non-mangrove features. The forest mask was created using an unsupervised (ISODATA) classification. Multiple classes were generated and then grouped in two larger classes: mangrove and non-mangrove areas. Figure 3 shows a false colour map of the study area after clouds and non-mangrove features were masked out. For comparison, a false colour image of the entire study area can be seen in Figure

20 (Appendix). Finally, bands were removed from the 126 band image using 3 criteria: high noise (especially in water absorption areas of the spectrum), radiometric errors such as negative reflectance values and differences in wavelength range between the SLC model and the HyMap sensor. A total of 13 bands were removed in the data preparation to leave 113 bands for data analysis.

2.3 Field Data and Processing

Field data was collected in August 2009 and August 2010 (Wandera, 2011). Chlorophyll measurements were made along 19 transects, from the coastline in an inland direction. Transects were positioned randomly throughout accessible areas of the delta due to inherent difficulties in navigating the mangrove environment. Transects were roughly 400 m. long with sample locations spaced at approximately 50 m. Positions were recorded using a handheld GPS receiver with positional accuracy (horizontal) of ±5-10 m. (Axelsson, 2011).

Chlorophyll was measured using a Minolta Inc. SPAD-502 Leaf Chlorophyll meter. Branches were collected from the upper part of a tree crown, from which 10 separate leaf measurements were made. The average value was calculated and assigned to the sample location (Wandera, 2011). A total of 66 sample points were used after some points were discarded due to masking of clouds and non-mangrove areas.

SPAD measurements are unitless values which are correlated with leaf chlorophyll and require an empirical formula for calibration to chlorophyll units ($\mu g\ cm^{-2}$). Calibration of field samples was carried out following field data collection. Empirical calibration equations are derived by regression analysis using the SPAD readings and laboratory derived chlorophyll measurements. Leaf samples are dissolved in a chemical solution to extract the chlorophyll and absorbance is measured using a spectrophotometer (Markwell et al., 1995; Richardson et al., 2002). Correlations are species specific and have been shown to also be dependent on leaf characteristics such as leaf thickness and leaf water content (Marenco et al., 2009). As the SPAD readings were the only vegetation data collected during the field sampling, an existing equation was chosen

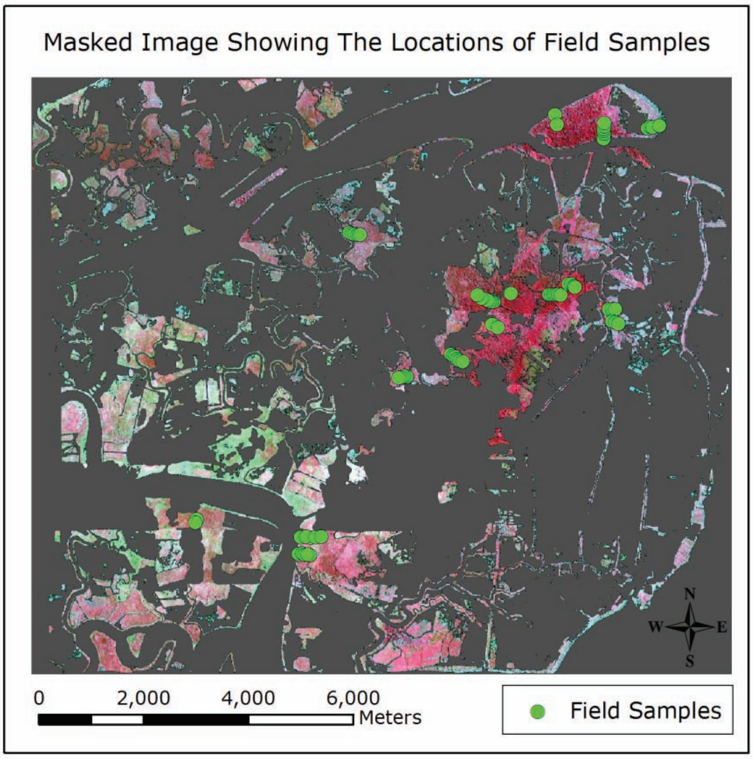

Figure 3: False colour infra-red image showing the areas covered by mangrove vegetation after clouds, water, shrimp ponds and other non-vegetation features were masked out. Chlorophyll field samples are highlighted in green.

for conversion to chlorophyll units. 3 available formulae were determined to be suitable for application to the mangrove field measurements. A formula by Coste et al. (2010), Equation 1, was developed using 13 tree species in tropical rainforest to reduce the species specific variations and have a wider range of applicability.

$$Chlorophyll = \frac{117.10*X}{148.84-X} \quad \text{(Equation 1)}$$

where *X* is the SPAD measurement and chlorophyll is in μg cm^{-2}.
Only one existing equation which was developed on a mangrove species could be found. The formula by Connelly (1997), Equation 2, was generated on *Rhizophora mangle* in the Caribbean.

$$Chlorophyll = \frac{X - 22.70}{0.57} \quad \text{(Equation 2)}$$

The formula developed by Richardson et al. (2002), Equation 3, was generated using measurements on *Betula papyrifera* (paper birch). This formula was found to provide reasonable calibration accuracy when applied to other species (Coste et al., 2010).

$$Chlorophyll = 5.52E - 04 + 4.04E - 04 * X + 1.25E - 05 * X^2 \quad \text{(Equation 3)}$$

A comparison was done to determine the differences between the three formulae. This was done by comparing the calibrated chlorophyll values, for each of the 66 field samples, using each of the 3 formulae.

2.4 Chlorophyll Estimation

2.4.1 Modelling

The Soil Leaf Canopy (SLC) model (Verhoef & Bach, 2007) was chosen in combination with the look up table inversion approach. SLC is a coupled model which includes a modified Hapke soil BRDF model, a robust PROSPECT leaf model and 4SAIL2, a modernised, hybrid canopy model. The model covers the spectral region between 400nm – 2400nm. Models of this type are suitable for representing a wider variety of canopies (Goel & Thompson, 2000), which was deemed important for modelling of the mangrove forest. The SLC model also includes simulation of soil moisture effects. The soil moisture conditions can be highly variable throughout the mangrove ecosystem depending on topography, tidal influx and river discharge. Reducing the uncertainty about the background reduces variation in the estimation of canopy parameters (Verhoef & Bach, 2007). Figure 5 shows the soil reflectance spectrum that was applied. The SLC model has generated good agreement between modelled and measured spectra when applied to other forest types such as beech and spruce. General agreement was also found with other models of similar type (Schlerf et al., 2007).

Simulated spectra for the LUT were generated by running the SLC model in forward mode with a pre-determined range of input parameters. The model has 22 input parameters of which 9 are known to have a significant effect on the reflectance of mangroves (Wandera, 2011). The range of input parameters was determined using sample spectra extracted from throughout the study area. SLCdemo, an implementation of the SLC model which allows manual adjustment of parameters, was used to invert these spectra manually. The results were used to define the range of values to be used for each of the 9 parameters. Table 1 lists the complete set of parameters used as input to the SLC model. The soil was assumed to be a Lambertian reflector. A simulated spectrum was then generated for each combination of parameters and stored together as the LUT (Mobley et al., 2005). Figure 4 shows an example of the resulting spectra.

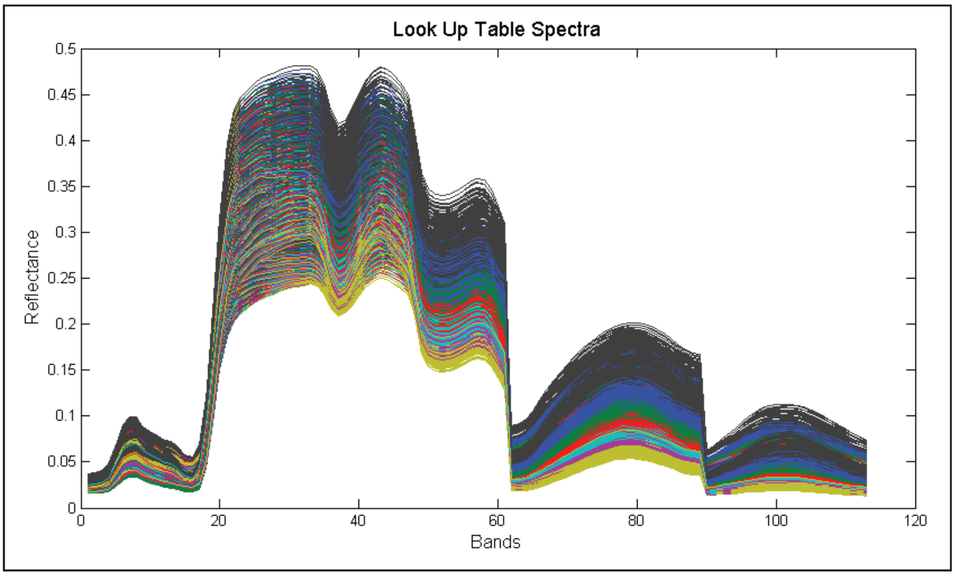

Figure 4: Visual representation of 50,000 simulated spectra stored in the LUT.

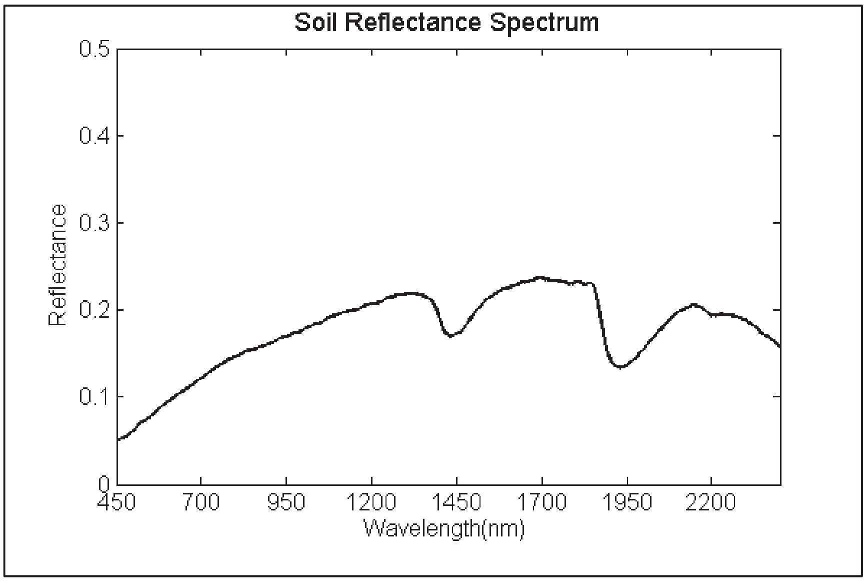

Figure 5: Reflectance spectrum applied for the soil background

Table 1: Table summarising the input parameters used for generation of the LUT

Parameter	Symbol	Min	Max	Steps	Constant
Leaf Parameters					
Chlorophyll a+b (green)	Cab	30	80	6	
Leaf Water Thickness (green)	Cw	0.02	0.08	7	
Leaf Dry Matter (green)	Cdm	0.001	0.009	5	
Leaf Senescence (green)	Cs	0.1	0.4	4	
Leaf Structure (green)	N	1.7	2.2	3	
Chlorophyll a+b (brown)	Cab_brown				10
Leaf Water Thickness (brown)	Cw_brown				0
Leaf Dry Matter (brown)	Cdm_brown				0.5
Leaf Senescence (brown)	Cs_brown				15
Leaf Structure (brown)	N_brown				10
Canopy Parameters					
Leaf Area Index	LAI	1.5	5	8	
Leaf Inclination Distribution	LIDFa				-0.35
Function	LIDFb				-0.15
Hot Spot	hot				0.05
Fraction of Brown Leaves	fB	0.03	0.05	2	
Layer Dissociation Factor	Diss				0.8
Vertical Crown Cover Percentage	Cv	0.75	0.85	3	
Tree Shape Factor	zeta	0.3	0.7	3	
Soil Parameters					
Soil Moisture	SM				0.25
External Parameters					
Solar Zenith Angle	tts				42
Observation Zenith Angle	tto				0
Relative Azimuth Angle	psi				157

2.4.2 Pixel-based Inversion

The reflectance spectrum was extracted for a pixel in which a field sample of chlorophyll was located. The spectrum was constructed by extracting the reflectance at that pixel from each band of the image data; subsequently referred to as the measured spectrum. The measured spectrum was then compared to the LUT entries (simulated spectra) by calculating the difference between measured and simulated spectra at every band. The difference between measured and simulated spectra was quantified using (Equation **4**.

$$Reflectance\ Difference = \sqrt{\sum_{i=1}^{n} \left(\frac{R(i)_{LUT(j)} - R(i)_{measured}}{R(i)_{LUT(j)}} \right)^2 \times w}$$

(Equation 4)

where R is the reflectance, i is the image band number, n is the total number of bands, j is the specific LUT entry and w is a weight matrix.

The LUT entry with the best matching spectrum was identified by the minimum reflectance difference value. The parameters used to generate that entry were then retrieved to obtain the predicted concentration of chlorophyll. Due to chlorophyll having its spectral response in the visible part of the spectrum, the weight matrix was used to increase the importance of bands in the visible to NIR region. This region was given a weight of 2, compared with the remaining bands weighted at 1. A higher value was not used as it would effectively disregard the remaining parts of the spectrum. Due to the heavy computing requirements of using a large LUT, both the modelled and measured data were reduced to fewer bands. Data in adjacent bands of hyperspectral data are highly correlated, meaning it was possible to discard several bands and retain most of the contained information. To keep data from across the spectrum, every fourth band was chosen; leaving 29 bands for data analysis. A comparison of the results showed that the same amount of variation could be explained by the 29 bands selected as with the total 113 bands. Validation was performed by comparing the estimated chlorophyll to the field measurements. RMSE, R^2 and a plot of measured vs. predicted chlorophyll were generated and used to assess the results.

2.4.3 Parameter Variation

Knowledge of the spatial variation of parameters was required to determine whether any of the 9 parameters could be assumed to have a constant value within neighbouring pixels in the image. To determine how the mangrove vegetation parameters varied within neighbourhoods, a combination of methods was used. Previous studies were reviewed to examine typical assumptions made with parameters and determine if any of these could be applicable to this study. Variations were also measured from the image data. Using the pixel-based inversion method, spectra from within a sample neighbourhood were extracted and inverted individually. The resulting parameter estimations were then compared across the neighbourhood and quantified by calculation of the coefficient of variation. This was repeated with varying window neighbourhood sizes. Several potential combinations of constant and variable parameters were tested by usage in the neighbourhood inversion method described in section 2.1.5, below. The combination that resulted in the highest accuracy was chosen.

2.4.4 Object Creation

To create image objects, a minimum noise fraction (MNF) image was created from the mosaic with non-mangrove areas masked out. The resulting eigenvalues were used to remove bands containing noise (Addink et al., 2007). The first 18 bands contained most of the information and the remaining MNF bands were discarded. This result was then used as the input for object creation. Objects were made using the segmentation algorithm in Trimble eCognition. Erdas Imagine Objective was also used to segment the image as a check of object quality. Using a spatial subset of the study area, the two results were compared visually on the basis of object shape and overlap to check for consistency. Only the result from eCognition was used in the object based estimation of chlorophyll. This was chosen due to its direct control of the object-scale parameter; which was of particular interest in this study and was successfully implemented in a previous, similar study (Addink et al., 2007).

The scale factor parameter was changed to examine its influence on the accuracy of the inversion results (Addink et al., 2007). The scale factor influences the size of the objects created and the number of pixels from which spectral information will be extracted for the inversion process. For the window based inversion, neighbourhood scale is controlled by the window size. In both software packages, low priority was given to any additional parameters such as object shape. This was done to allow objects to be created based on the spectral information.

2.4.5 Neighbourhood Inversion

Inversion to include spectral information from neighbouring pixels took place in two stages. A spatial neighbourhood was first identified, which included the location of a chlorophyll field sample. The spectrum for each pixel within the window was extracted and the average spectrum was calculated. The average neighbourhood spectrum was inverted as with the pixel-based method, to identify a parameter combination that minimises RMSE in all the neighbourhood pixels. For the parameters which have been identified as having negligible variation within the neighbourhood, this solution is kept for all pixels in the neighbourhood. The remaining parameters are allowed to vary from pixel to pixel.

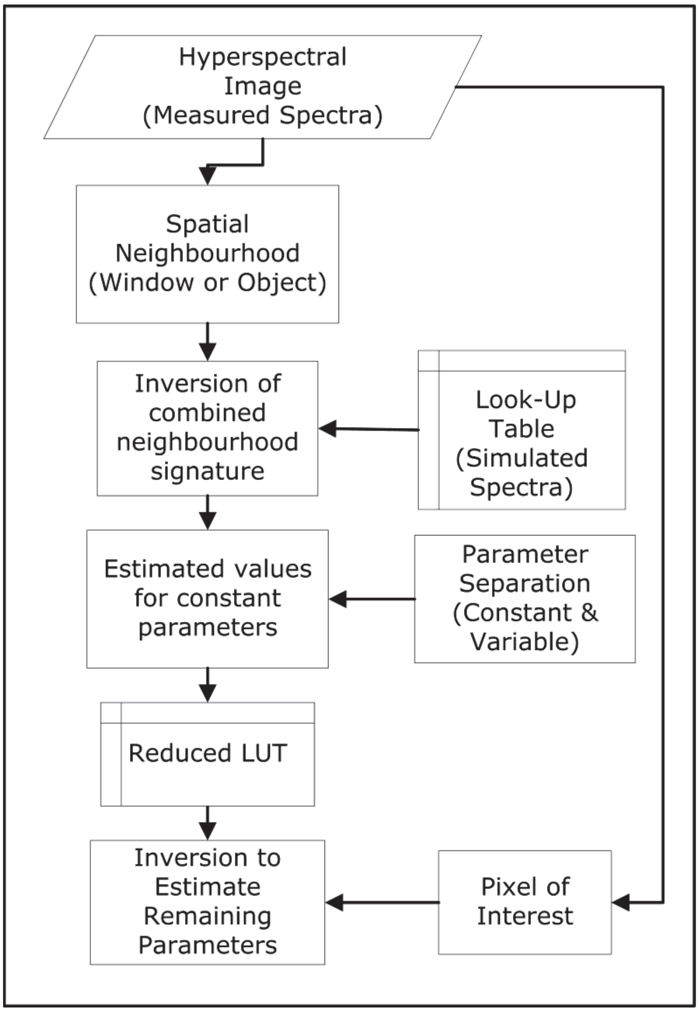

Figure 6: Flowchart of the neighbourhood inversion method

For the second stage, the LUT was reduced to contain only entries that were generated using the combination of constant parameters previously determined. The spectrum of only the pixel of interest (pixel where the field sample was located) was then extracted and inverted using the reduced LUT to obtain estimated values for the remaining parameters. This procedure was repeated using two neighbourhood identification methods. Sliding window neighbourhoods were created using a square overlay, with the pixel of interest always at the center. Object neighbourhoods were identified by areas created through the image segmentation process described previously (2.1.4). The pixel of interest in this neighbourhood was not fixed relative to the object and varied for each object. A flowchart of the neighbourhood inversion method is shown in Figure 6.

2.4.6 Validation and Map Generation

Validation of results was performed using a number of statistical measures. A total of 66 field samples of chlorophyll were used to calculate RMSE and R^2 values when compared with estimated chlorophyll. A Wilcoxon rank sum test was also used to test whether there was a significant difference between chlorophyll estimates retrieved using the pixel based method and each of the neighbourhood based methods. Tests were performed at significance level $\alpha = 0.10$.

Maps of chlorophyll predictions were created by applying both prediction methods across the study area. The large LUT size and high spatial resolution of the image resulted in very slow map generation times. Therefore only a spatial subset of the study area was generated. The north-east quadrant was selected because it was considered representative of the study area; containing a mixture of large mangrove stands, smaller fragmented mangrove areas, man-made ponds, natural drainage features and it also contained most of the field samples. Although the accuracy estimates obtained apply directly to the generated maps, a test of spatial autocorrelation of the chlorophyll field samples was also performed. This served as a tool for assessing any observed spatial variations.

3. Results

3.1 Field Data Calibration

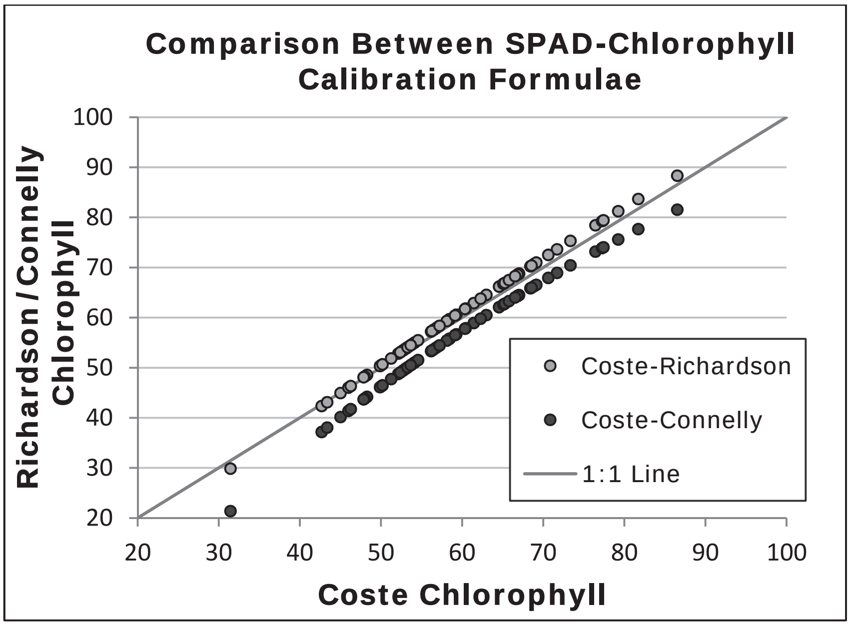

Figure 7: Graph showing the comparisons between different SPAD to chlorophyll calibration formulae at the 66 sample locations.

The results of the comparison between different SPAD calibration formulae can be seen in Figure 7. The Coste and Richardson formulae consistently produce very similar chlorophyll values. The average difference was 1.2 µg cm^{-2} and maximum difference was 2.0 µg cm^{-2}. The Coste and Connelly comparison shows a small systematic difference at all sample points; with the Coste formula always giving a higher calibration value. The average difference was 3.3 µg cm^{-2} and maximum difference of 10.0 µg cm^{-2}.

3.2 Pixel Based Estimation

Application of the pixel based inversion approach resulted in relative RMSE of 31.5% and R^2 of 28.9%. This result is similar to that of the previous study in this area, which achieved relative RMSE of 27.5% and R^2 of 30% (Wandera, 2011). Figure 8 shows the comparison plot of measured and predicted chlorophyll. Points appeared in a wide cluster with a fairly even distribution above and below the 1:1 line. Figure 9 shows the resulting spectra matches for two of the sample points. M0303 (top) was a point that was predicted well with measured and predicted chlorophyll at 53 and 50 μg cm^{-2} respectively. M2505 (bottom) achieved a less accurate prediction with measured chlorophyll of 56 μg cm^{-2} and predicted chlorophyll of 30 μg cm^{-2}. Both points achieved a relatively good match between measured and simulated spectra.

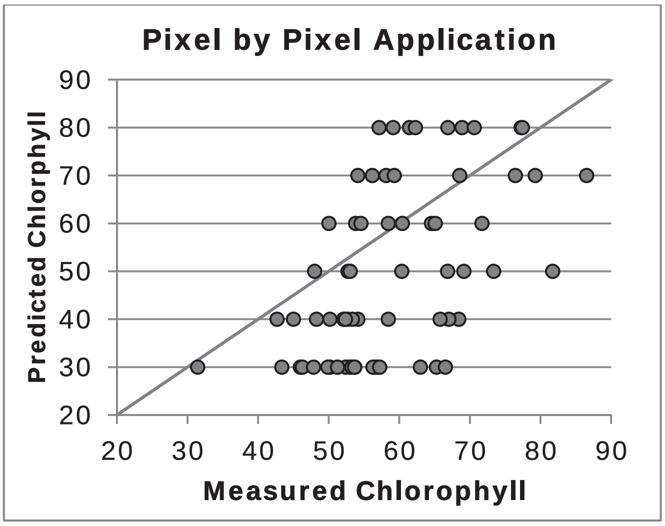

Figure 8: Graph showing the comparison between measured and predicted values for the 66 sample locations using the pixel-based inversion method.

3.3 Parameter Variation and Object Comparison

From previous studies, a number of parameters were identified which are typically assumed to have negligible intra-neighbourhood variation. These include Cab, Cdm, N and hot spot. The main variation within neighbourhoods is attributed to LAI (Atzberger, 2004; Atzberger & Richter, 2009).
Figure 10 shows the results of measuring the variation of parameters from the image data. Some disagreement can be seen, with Cdm showing the highest variations and LAI having relatively low variation within the neighbourhood. A combination of 4 parameters was found to produce the highest accuracy chlorophyll estimation when kept constant. Crown cover percentage (Cv), leaf water thickness (Cw), leaf senescence (Cs) and leaf structure (N). All other parameters were allowed to vary within the spatial neighbourhood.

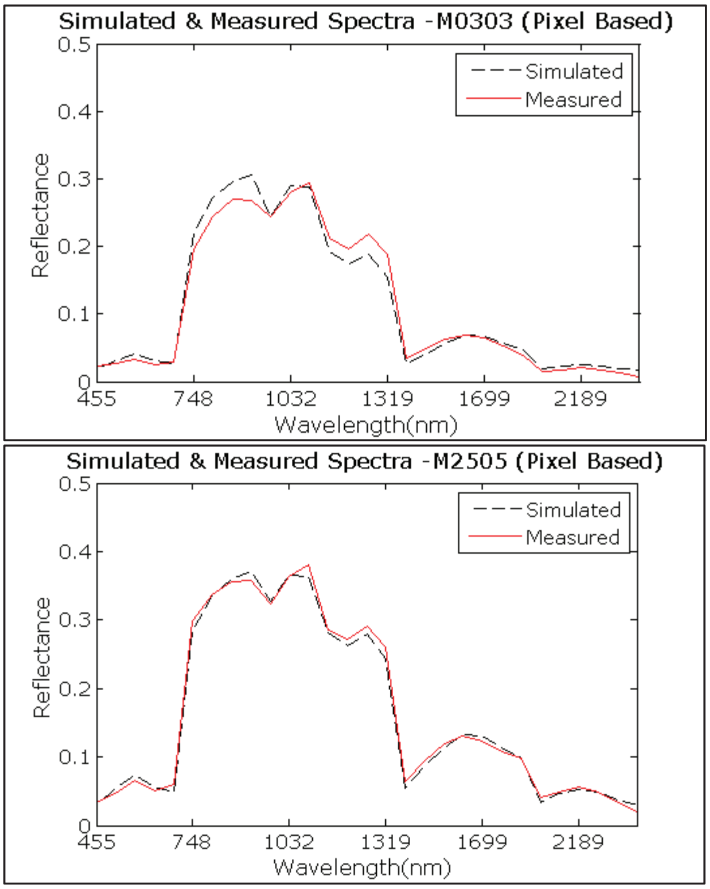

Figure 9: Comparison between simulated and measured spectra at sample points M0303 and M2505. The simulated spectrum was selected as the best match for the sample locations using the pixel based method.

Figure 11 shows the results of image segmentation to create objects. The different software produced comparable results to some extent. Objects were generally created at the same location in each image and also approximately the same size. eCognition produced objects with straight, square boundaries whereas Imagine Objective produced more irregular shaped objects. Differences can be seen most in the south-east area of the image, where eCognition creates large objects over a fairly homogeneous background and Imagine Objective creates a mixture of both large and very small objects.

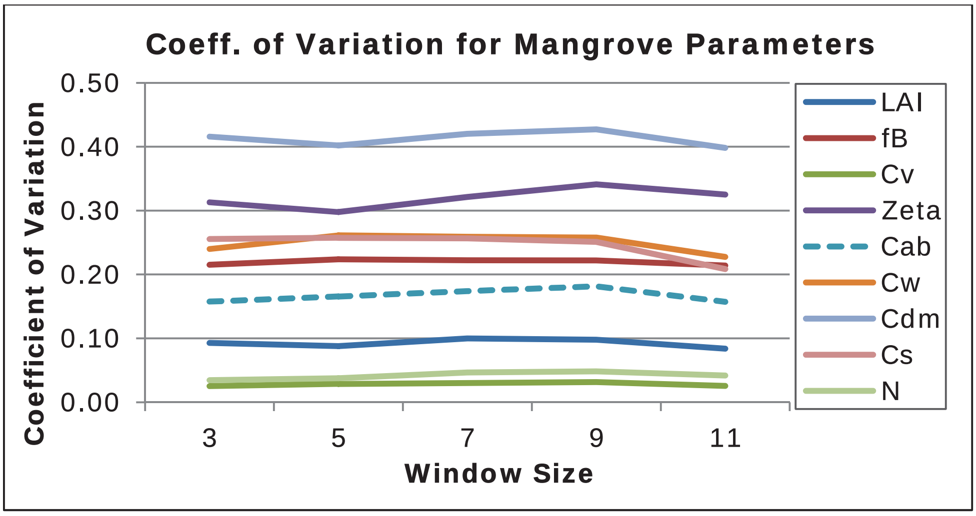

Figure 10: Plot showing the coefficient of variation measured from image data, within different window sizes for each of the 9 input parameters.

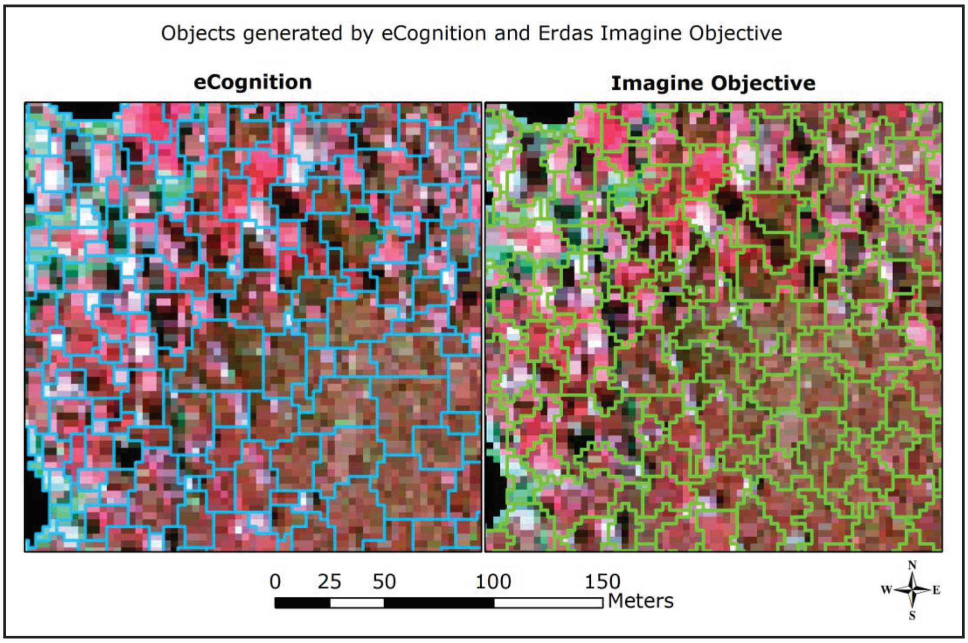

Figure 11: Images showing the comparison between objects created by eCognition (left) and Imagine Objective (right). eCognition objects shown were created with a scale factor of 3.

3.4 Neighbourhood Based Estimation

The neighbourhood inversion results using a 3x3 window showed a small iincrease in the accuracy of chlorophyll prediction. RMSE was approximately the same and R^2 showed a little more explained variation. Changing the neighbourhood size for the window-based method resulted in small changes in R^2, while the RMSE values remained fairly constant. A comparison of the different window sizes is shown in Table 2.

Objects with scale factor 2 produced objects of similar size to the 3x3 window, however the resulting chlorophyll predictions do not show a similar improvement. Change of object scale shows variations in both RMSE and R^2 values, with R^2 values increasing up to scale factor 5. Table 3 contains a comparison of the results obtained from different sized objects. Objects with scale factor 5 produced approximately the same results as the window based application with 3x3 window size. Plots of measured and predicted chlorophyll are shown in Figure 12 and Figure 13 for a 3x3 window and scale factor 2 objects respectively. Window and object neighbourhoods resulted in similar plots when comparing measured and predicted chlorophyll. Only small differences could be observed between the plots, with both neighbourhood inversion methods showing a similar trend and distribution of points to the pixel-based method. The results of the Wilcoxon rank sum tests showed that the differences observed between the pixel based results and the neighbourhood based methods were not significant for any of the neighbourhood sizes. For this significance test, p-values would have had to be less than 0.1 to indicate a significant difference between the two sets of estimated values.

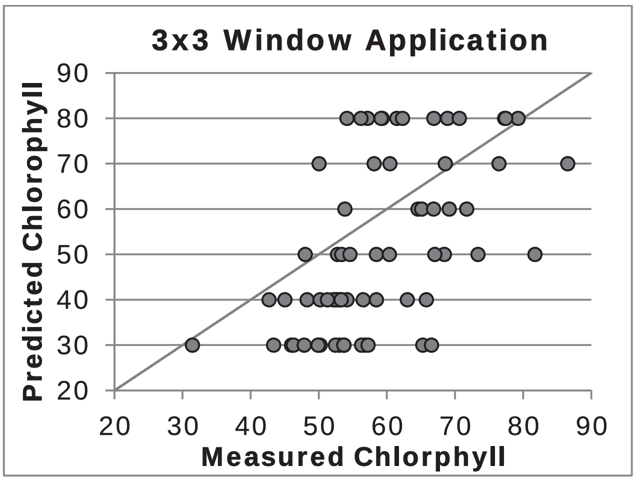

Figure 12: Graph showing the comparison between measured and predicted chlorophyll using a 3x3 window-based inversion method.

Table 2: Table summarising the results of changing window size with a window-based inversion.

Window Size	3x3	5x5	7x7	11x11	15x15
RMSE (µg cm^{-2})	17.07	17.18	17.04	16.92	17.04
Rel. RMSE (%)	30.99	31.19	30.94	30.72	30.93
R^2 (%)	30.38	28.33	28.50	28.04	28.85
p-value	0.5262	0.5838	0.5509	0.5010	0.5900

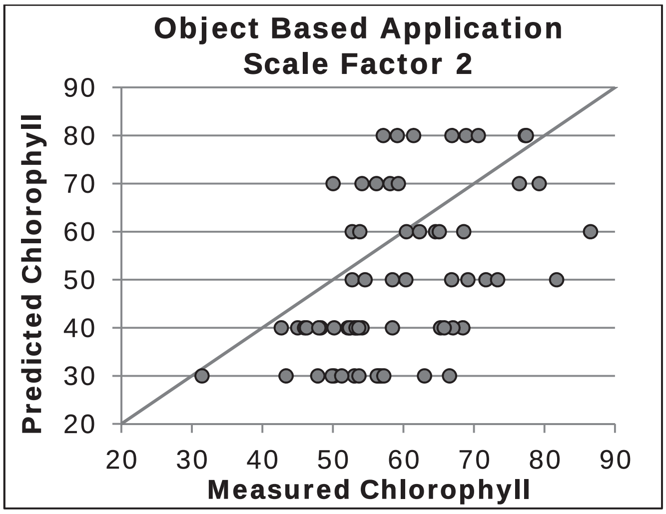

Figure 13: Graph showing the comparison between measured and predicted chlorophyll using and object-based inversion method. Objects were created at scale factor 2.

Table 3: Table summarising the results of different scale factors using an object-based inversion.

Object Scale	2	3	4	5	7
RMSE (µg cm^{-2})	15.85	19.38	15.49	17.89	15.50
Rel. RMSE (%)	26.35	33.14	25.75	30.61	25.77
R^2 (%)	24.87	24.70	27.23	30.19	27.80
p-value	0.8254	0.7129	0.7327	0.9204	0.8837

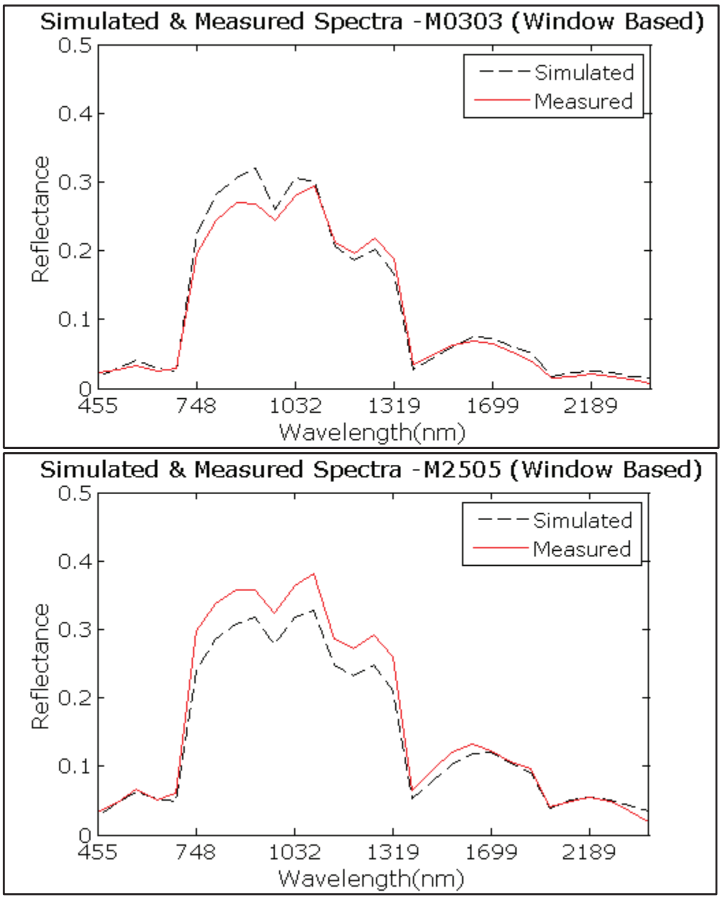

Figure 14: Comparison between simulated and measured spectra for two field sample locations. The simulated spectrum shown is the closest match selected from the LUT using the window based approach. M0303 (top) achieved a good prediction while M2505 (bottom) had a poor prediction.

Examples of the best fit spectra selected by the neighbourhood inversion approach are shown for two sample locations, in Figure 14. The LUT entries chosen for both samples were different to the spectra chosen in the pixel based approach; however the estimated chlorophyll values were the same. The spectra within the spatial neighbourhoods at these two samples were also extracted. Figure 18 (Appendix) shows a comparison between spectra extracted for each pixel within 3x3 window neighbourhoods and Figure 19 (Appendix) shows the spectra extracted from each pixel within the objects generated at scale factor 2, at the same sample locations. In both the window and object neighbourhoods, the spectra at M0303 were closely grouped and the spectra at M2505 show a wide range of variation. At M0303, with the pixel of interest was located centrally within the range of variation, whereas at M2505, the pixel of interest is close to the edge of the range.

3.5 Chlorophyll Maps

Figure 16 and Figure 17 show the output maps after the pixel based and object based inversion approaches were applied to the study area. The two maps appeared almost identical with no clear differences in the spatial variation of chlorophyll. Small areas of mangrove, such as fringe bands that occur along ponds, display low to average concentrations of chlorophyll. In larger mangrove stands, low concentrations were generally observed in close proximity to ponds. The two largest areas of continuous mangrove forest occur at the center of the map and the island to the north; both areas exhibit high concentrations. Exceptions to these trends occur south of the island. Two small patches of mangrove exhibit high concentrations of chlorophyll, compared to other patches of similar size which generally showed low to average concentrations. A clear line or break was observed through the large forest area at the center. This appeared to be an artifact occurring at the boundary between two image strips. The semi-variogram of chlorophyll (Figure 15) shows evidence of weak spatial autocorrelation. A low sill can be observed occurring at a range of approximately 100 m.

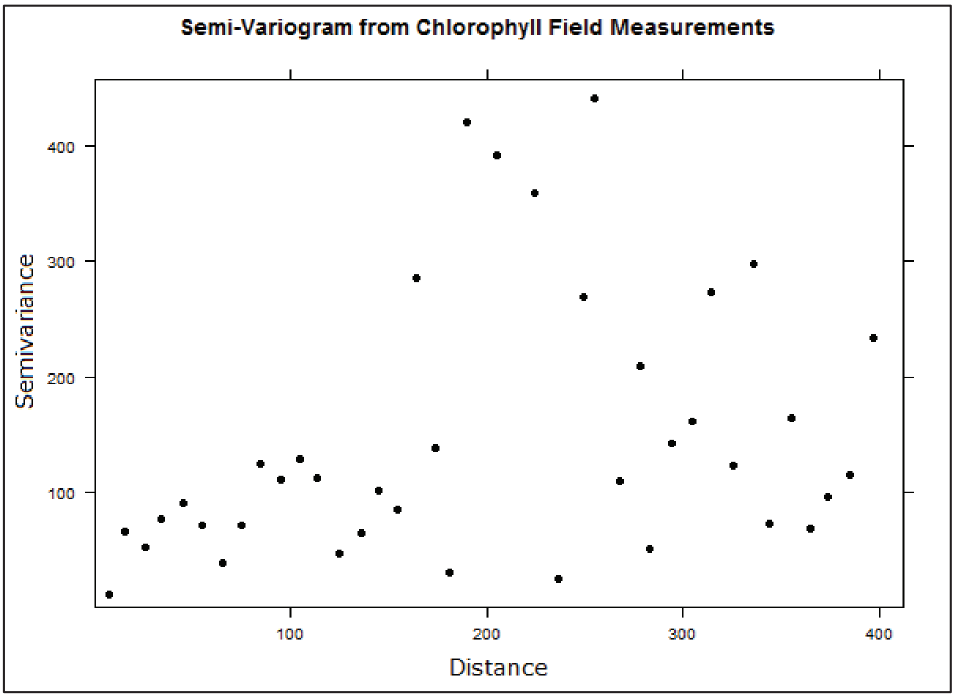

Figure 15: Semi-variogram constructed using field measurements of chlorophyll

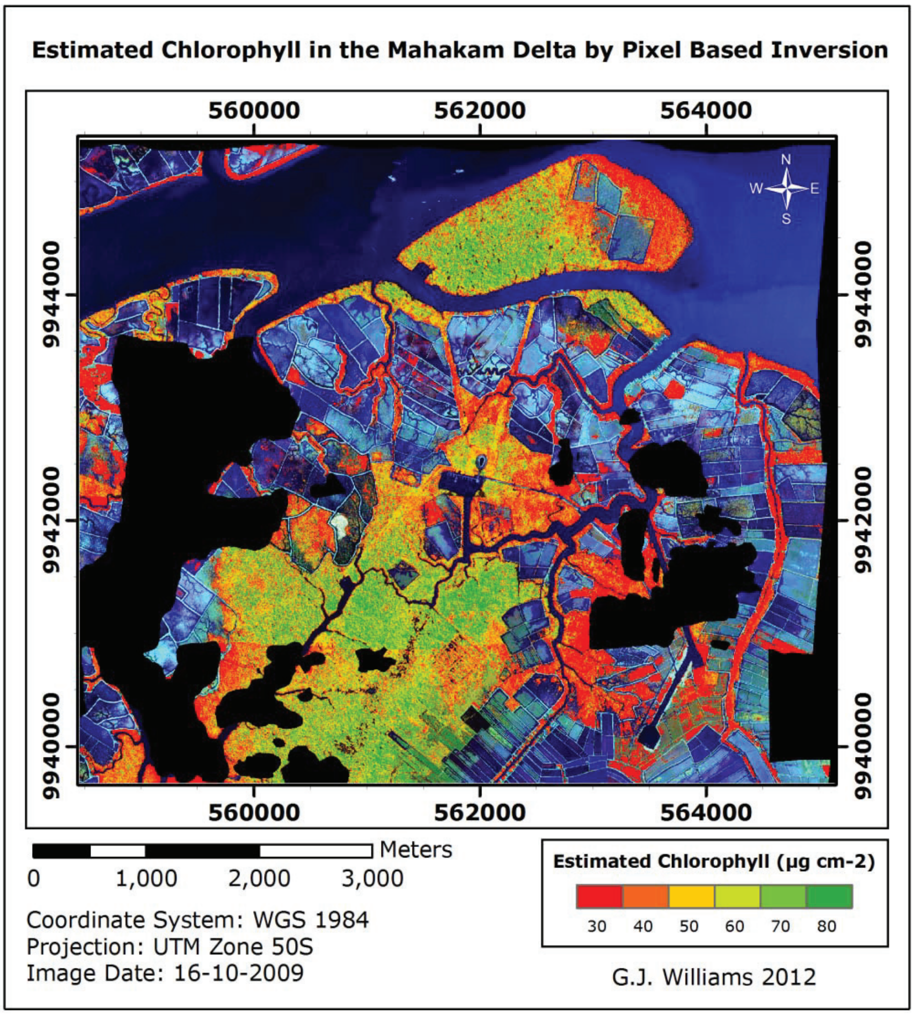

Figure 16: Map of chlorophyll in the Mahakam delta, estimated using the pixel based inversion approach. Predictions are overlaid on a false colour composite of the study area to show the presence of shrimp ponds and other features.

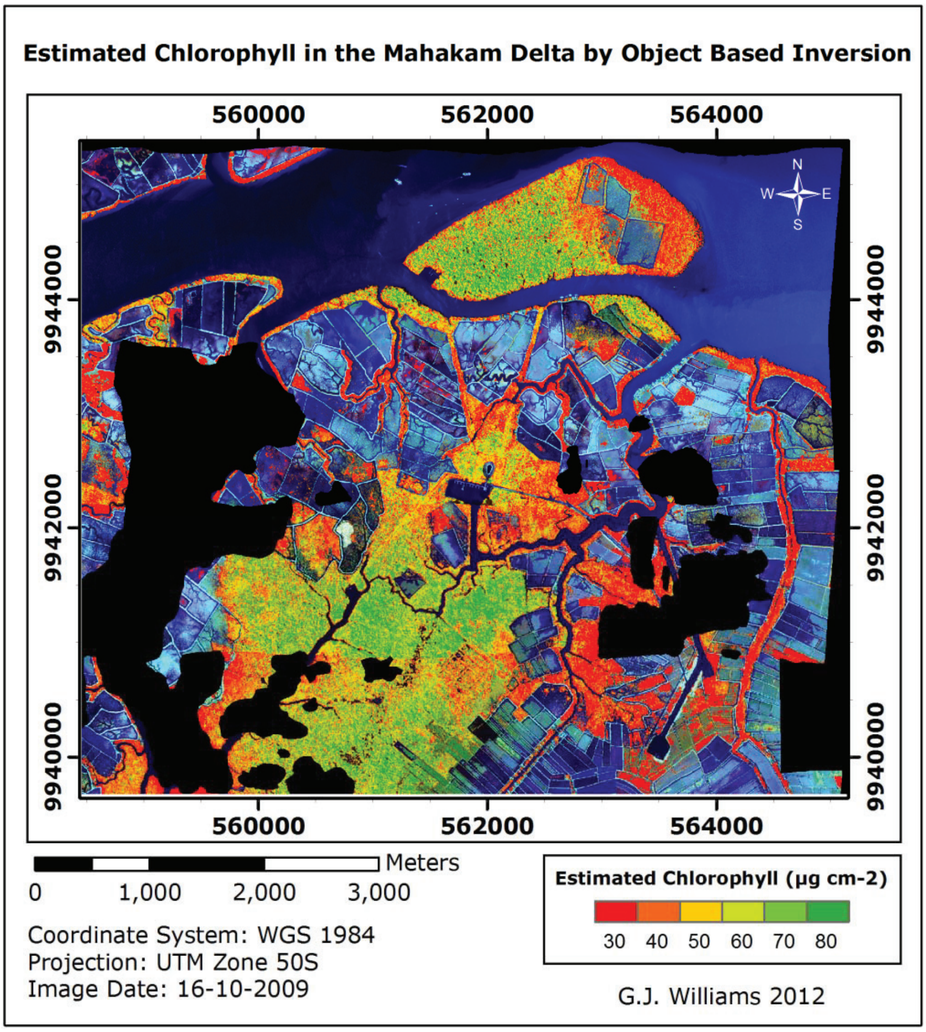

Figure 17: Map showing the estimated chlorophyll in the Mahakam delta. Chlorophyll was estimated using the object based inversion approach and is overlaid on a false colour composite of the study area.

4. Discussion

The results have shown that the neighbourhood based inversion approach has not been able to significantly improve the accuracy of the pixel based inversion. The neighbourhood approach, which includes spectral information from surrounding pixels, produced approximately the same results achieved by inversion of individual pixels. The lack of improvement highlights the occurrence of underlying issues which may have contributed to the poor results. The pixel based and neighbourhood based approaches produced very similar plots of measured chlorophyll against predicted chlorophyll. The clustering of points around the 1:1 line shows that predicted chlorophyll have the correct order of magnitude and there are no large systematic errors affecting the results. However, the even distribution of points above and below the line indicates the possible influence of a random error within the data analysis.

The smallest window size (3x3) used in the window based inversion resulted in the highest accuracy. When window size was increased, the resulting R^2 was lower but approximately the same for all the subsequent sizes, 5x5 to 15x15. As a result, the window approach showed no correlation between accuracy and window size. With objects, a small trend was observed with R^2 values increasing with increase in scale, up to scale factor 5. The two neighbourhood inversion methods show contrasting results. The two neighbourhood identification methods achieved approximately the same maximum accuracy, but with neighbourhood sizes that were considerably different. Both sets of results present plausible scenarios. If noise exists in the image data, the best results could be achieved using small neighbourhoods as seen in the window based approach. However, increasing neighbourhood size means there is contribution of more spectral information from surrounding pixels, as seen with the object based approach. Given that the accuracies of both methods are relatively low, it is difficult to make specific conclusions on the relationship between neighbourhood scale and accuracy.

The comparison between software for object creation showed general agreement in the resulting objects. Objects were created at the same locations and with a similar number of pixels. The main difference observed was the object shape and consistency of object size in some parts of the image. The aim of this comparison was to ensure that objects were created in a robust manner. Some variation was expected due to differences in software implementation and segmentation algorithms (Meinel & Neubert, 2004). The agreement found was therefore considered sufficient to apply the objects to the inversion method. Differences between software and the segmentation results were not compared further.

Upon inspection of the results, a number of errors were identified which may have contributed to the low accuracies obtained by the pixel based and neighbourhood based approaches. Table 4 shows a summary of the errors affecting the inversion methods. Examination of the reflectance of pixels within a neighbourhood shows that it is possible to have large variations in reflectance between adjacent pixels over a small area (Figure 18 and Figure 19 in Appendix). This can be explained by the heterogeneous nature of mangrove forests, which would result in mixed pixels. A scene containing mangrove vegetation may contain different tree ages, soil background and differences in canopy density (Hogarth, 2007). In areas where spectral variations are high, including information from these pixels would not be contributing to the prediction but instead increasing uncertainty. These factors may be amplified by the radiometric variations that were observed. The small variations in reflectance could only be observed in areas of image overlap. These variations were considered negligible and can be a result of differences in viewing angle. Areas of image overlap are at the edge of the sensor swath and therefore these areas have been viewed at an extreme angle from each of the adjacent flight lines. Both sources of uncertainty, the mangrove environment and image noise, would vary across the study area. They could therefore contribute to the random error observed in the results.

Table 4: Summary of errors in the data analysis that may influence the accuracy of the pixel and neighbourhood inversions.

Uncertainty in Pixel and Neighbourhood Methods	**Uncertainty in Neighbourhood Method Only**
Radiometric variations	Large variation in reflectance within neighbourhoods - heterogeneity of mangrove environment
Positional uncertainty of field samples	
Calibration of field measurements	Uncertainty of parameter assumptions and applicability over study area.
Simplifications of modelling and inversion	
Time difference between image and field samples	
Field sample representation of image pixels	

For the first stage of the neighbourhood inversion, it was necessary to identify parameters that can be assumed to have negligible variation over a small area. No measurements of canopy or foliar parameters were made, apart from the chlorophyll field measurements. Identifying the behaviour of the parameters within neighbourhoods therefore had to be carried out in an experimental manner with reliance on image data and chlorophyll measurements for these results. Assumptions from other studies were also used, however these were based on studies in agricultural areas, representing more ideal and uniform growing conditions than the mangrove environment (Atzberger, 2004; Atzberger & Richter, 2009). Some agreement and disagreement was seen between the two approaches. The leaf structure parameter (N) and leaf dry matter (Cdm) were identified in previous studies to have negligible variation within neighbourhoods. Measuring from the image, N also showed very little variation but Cdm had high variation. Cdm may be explained by the evergreen nature of most mangrove species. The process of leaf fall, nutrient resorption and new leaf growth are continuous processes which may lead to higher variations in leaf parameters (Hogarth, 2007; Tomlinson, 1994). The best combination of parameters determined from the image means that the final combination chosen is not necessarily the true behaviour of parameters in the mangrove forest. Any noise or artifacts that exist in the data would influence the results. The ill-posed problem also exists as the pixel based inversion method was used for obtaining parameter estimates within the neighbourhood. The combination that was used is therefore the parameter combination that provided the best results with the available data. The study area and mangrove environments in general, are known to consist of multiple species and variations of physical conditions. This means that the combination most accurately representing the spatial variation of parameters within neighbourhoods may also vary across the study area.

The estimated geometric accuracy of the image data agreed with the known accuracy estimate for the handheld GPS receiver that was used. Geometric correction of the image was estimated at 6-9 m. while the GPS receiver had an accuracy of 5-10 m. Assessing the accuracy of the image correction was carried out in open areas with little or no overhead cover. It was therefore expected that when sample locations were observed within the mangrove forests, positional accuracy may be lower. As the image had a high spatial resolution, positional uncertainty increases the likelihood of a measured sample occurring in a different pixel or neighbourhood to the one being inverted. With the positional error being dependent on the site specific canopy cover, the magnitude of this error would vary at every sample point.

The calibration of chlorophyll field measurements may also introduce some uncertainty to the results. The lack of concurrent laboratory testing or mangrove based calibration formulae means that it was not possible to verify the accuracy of the calibrated chlorophyll values. The Connelly formula was the only dedicated calibration formula for a mangrove species. Previous studies on other plant species have shown, however, that the relationship between SPAD readings and leaf chlorophyll is non-linear (Markwell et al., 1995). This suggests that the Connelly model approximated the true relationship to a linear model. The Coste model was deemed appropriate because it was based on multiple tropical forest species, therefore having a generalised applicability. This was important due to the nature of the study area, consisting of multiple mangrove species. Although the 3 available formulae were developed on different species, differences between them were found to be relatively small (Figure 7). The similarity between them shows that choosing an incorrect formula will contribute a small error to the final accuracy estimation.

The final results also contain inherent errors from the physical model and inversion approach. The SLC model is complex and was formed through a combination of several sub-models. As all models contain some error, SLC could not perfectly simulate the mangrove spectra. However, comparison of spectra showed that the model performed well, producing simulations that closely matched the measured spectra. The LUT method implemented also introduces some error as it only allowed chlorophyll values to be chosen at the interval specified in the LUT generation (Goel & Thompson, 2000). In the LUT used, chlorophyll was input at an interval of 10 $\mu g\ cm^{-2}$ and could not be reduced due to the limitations imposed by LUT size and the resulting processing time. To be applicable for the entire study area, the LUT had to contain simulated spectra representative of the environmental conditions occurring in nature (Mobley et al., 2005). Since these conditions were found to be varied, several of the model parameters required multiple steps over a large range.

An error that may contribute to the low accuracy obtained is the use of field data collected in August 2010. Given that the study area is known to have a high rate of environmental change, leaf chlorophyll concentrations measured after 1 year may be different to the actual chlorophyll at the image date. It was noted that points with a large error occurred in both the 2009 and 2010 datasets. To examine the effect of using points from 2010, validation of pixel based, sliding window (3x3) and object (scale factor 2) inversions were repeated using only sample points from 2009. In each case, a substantial change in RMSE and R^2 was not observed. The R^2 value decreased for the window method and increased for objects but in both cases the change was approximately 1%. It is expected that the time lag in the collection of field data contributes some uncertainty; however the available evidence suggests that it is not the sole contributing error.

An additional consideration of the field samples is whether they are representative of the image pixels. Multiple measurements were made on leaves from a branch at the top of the canopy. These were then averaged to a single value. The distribution of field samples shows that samples were generally taken in areas of dense, continuous forest where tree crowns may overlap. In these areas the chance of mixed pixels is high. Field samples therefore lacked redundant observations spread over the area of one image pixel. Given that radiation can be reflected from the top of canopy as well as lower layers, observations at lower canopy levels are also absent.

The errors identified are spread throughout the data analysis. As a result, propagation of error may also occur. The quantification of some of the errors was therefore useful. This highlights the relative contribution of errors and indicates where improvement may be required to improve the quality of the result (Heuvelink, 1998). The number of uncertainties relating to the field samples indicates that they may be the most significant source of error.

The poor inversion results achieved and the errors identified mean that the accuracies of the associated chlorophyll maps are also low. The maps therefore cannot be used for the estimation of chlorophyll content at specific locations. It may still be possible however, to extract relevant information from them. Agreement between the maps generated through 2 different approaches indicates that the methods have been able to identify the spatial variations that occur. This is supported by the range of spatial autocorrelation observed in the field samples. Rapid changes in chlorophyll within a short space occur only at the flight line artifacts previously identified. The maps can therefore be used to examine general trends of how chlorophyll varies throughout the study area. A preliminary observation can be made that mangrove areas that exist near to shrimp ponds have low chlorophyll content. However, these areas occur close to the coast, where the environment is more exposed to tidal cycles. Greater exposure to tidal variations would result in the flushing of available nutrients. Also, in large, undisturbed forest areas, chlorophyll content appears much higher. Maps based on more accurate results would allow the observation of spatial variations to be made with greater certainty as quantitative variations could also be examined.

5. Conclusion

Application of the neighbourhood based inversion to predict chlorophyll was not able to significantly improve the results achieved by the pixel based approach. Neighbourhoods were defined in two ways, sliding windows and objects, from which contrasting results were obtained. Varying the neighbourhood size revealed that sliding windows achieved highest accuracy with 3x3 windows (Rel. RMSE=30.99% and R^2=30.38). The object based approach achieved highest accuracy with scale factor 5 (Rel. RMSE=30.61% and R^2=30.19%). Due to differing trends between neighbourhood size and accuracy and the relatively low accuracy, no conclusive relationship could be identified.

To implement the neighbourhood based inversion, vegetation parameters with negligible variation within neighbourhoods had to be identified. 4 parameters were found to exhibit little variation over a small area: Cv, Cw, Cs and N. Given that no field samples of additional parameters were made, these parameter variations could only be measured from the image directly. The selected combination may therefore be influenced by variations in the image rather than true parameter variations.

Comparisons between measured and predicted chlorophyll revealed similarities between the pixel based and neighbourhood based approaches. Assessment of the data analysis highlighted several sources of error in the input data. Some of the errors could be quantified to provide an estimate of their relative contribution in the case of error propagation. However, multiple errors were associated with the chlorophyll field samples that were collected. Consequently, these uncertainties indicated that the field samples may not be representative of the image pixels both in terms of position and chlorophyll content.

The low accuracy achieved by the pixel based and neighbourhood based inversions mean that the resulting chlorophyll maps also have a low accuracy. The maps therefore should not be used to estimate chlorophyll concentrations at specific locations. The consistent spatial structure within the images shows that they can be used to examine general trends of chlorophyll variation throughout the study area.

5.1 Recommendations

For future studies, it is recommended that more rigorous field procedures are implemented. The nature of the mangrove environment makes field sampling inherently difficult. However, sampling methods should be specifically suited to the environment to ensure accurate, representative samples are obtained.

Approaches outlined by Combal et al. (2003) and Atzberger (2004) may be combined, using a combination of a priori information of canopy characteristics and a spatially constraint inversion. Uncertainties still exist regarding how vegetation parameters vary within the mangrove canopy. Future studies should aim to collect samples of multiple parameters to obtain more substantial evidence for the spatial variation of parameters.

References

Addink, E. A., De Jong, S. M., & Pebesma, E. J. (2007). The importance of scale in object-based mapping of vegetation parameters with hyperspectral imagery. *Photogrammetric Engineering and Remote Sensing, 73*(8), 905-912.

Atzberger, C. (2004). Object-based retrieval of biophysical canopy variables using artificial neural nets and radiative transfer models. *Remote Sensing of Environment, 93*(1-2), 53-67.

Atzberger, C., & Richter, K. (2009). *Geostatistical regularization of inverse models for the retrieval of vegetation biophysical variables.* Paper presented at the Remote Sensing for Environmental Monitoring, GIS Applications and Geology IX, Proceedings of SPIE Vol. 7478.

Axelsson, C. R. (2011). *Predicting mangrove leaf chemical content from hyperspectral remote sensing using advanced regression techniques.* Unpublished MSc Thesis, University of Twente Faculty of Geo-Information and Earth Observation ITC, Enschede.

Carter, G. A., & Spiering, B. A. (2002). Optical Properties of Intact Leaves for Estimating Chlorophyll Concentration. *Journal of Environmental Quality, 31*(5), 1424-1432.

Combal, B., Baret, F., Weiss, M., Trubuil, A., Macé, D., Pragnère, A., et al. (2003). Retrieval of canopy biophysical variables from bidirectional reflectance: Using prior information to solve the ill-posed inverse problem. *Remote Sensing of Environment, 84*(1), 1-15.

Connelly, X. M. (1997). The use of a chlorophyll meter (SPAD-502) for field determinations of red mangrove (*Rhizophora mangle* L.) leaf chlorophyll amount. *NASA University Research Centers Technical Advances in Education, Aeronautics, Space, Autonomy, Earth and Environment, 1*, 198-190.

Coste, S., Baraloto, C., Leroy, C., Marcon, E., Renaud, A., Richardson, A. D., et al. (2010). Assessing foliar chlorophyll contents with the SPAD-502 chlorophyll meter: a calibration test with thirteen tree species of tropical rainforest in French Guiana. *Annals of Forest Science, 67*(6).

Darvishzadeh, R., Skidmore, A., Schlerf, M., & Atzberger, C. (2008). Inversion of a radiative transfer model for estimating vegetation LAI and chlorophyll in a heterogeneous grassland. *Remote Sensing of Environment, 112*(5), 2592-2604.

Dutrieux, E. (1991). Study of the ecological functioning of the Mahakam delta (East Kalimantan, Indonesia). *Estuarine, Coastal and Shelf Science, 32*(4), 415-420.

FAO. (2007). *The World's Mangroves 1980-2005*. Rome (Italy): Food and Agriculture Organisation of the United Nations.

Goel, N. S., & Thompson, R. L. (2000). A snapshot of canopy reflectance models and a universal model for the radiation regime. *Remote Sensing Reviews, 18*(2-4), 197-225.

Goodenough, D. G., Li, J. Y., Asner, G. P., Schaepman, M. E., Ustin, S. L., Dyk, A., et al. (2006). Combining hyperspectral remote sensing and physical modeling for applications in land ecosystems. *2006 IEEE International Geoscience and Remote Sensing Symposium, Vols 1-8* (pp. 2000-2004). New York: IEEE.

Haboudane, D., Miller, J. R., Tremblay, N., Zarco-Tejada, P. J., & Dextraze, L. (2002). Integrated narrow-band vegetation indices for prediction of crop chlorophyll content for application to precision agriculture. *Remote Sensing of Environment, 81*(2-3), 416-426.

Held, A., Ticehurst, C., Lymburner, L., & Williams, N. (2003). High resolution mapping of tropical mangrove ecosystems using hyperspectral and radar remote sensing. *International Journal of Remote Sensing, 24*(13), 2739-2759.

Heuvelink, G. B. M. (1998). *Error Propagation in Environmental Modelling with GIS*. London: Taylor & Francis.

Hogarth, P. J. (2007). *The biology of mangroves and seagrasses* (Second ed.). New York: Oxford University Press.

Huber, S., Kneubuhler, M., Psomas, A., Itten, K., & Zimmermann, N. E. (2008). Estimating foliar biochemistry from hyperspectral data in mixed forest canopy. *Forest Ecology and Management, 256*(3), 491-501.

Li, X., & Strahler, A. H. (1986). Geometric-Optical Bidirectional Reflectance Modeling of a Conifer Forest Canopy. *IEEE Transactions on Geoscience and Remote Sensing, GE-24*(6), 906-919.

Liang, S. (2005). *Quantitative remote sensing of land surfaces* (1st ed.). New Jersey: Interscience.

Marenco, R. A., Antezana-Vera, S. A., & Nascimento, H. C. S. (2009). Relationship between specific leaf area, leaf thickness, leaf water content and SPAD-502 readings in six Amazonian tree species. *Photosynthetica, 47*(2), 184-190.

Markwell, J., Osterman, J. C., & Mitchell, J. L. (1995). Calibration of the Minolta SPAD-502 leaf chlorophyll meter. *Photosynthesis Research, 46*(3), 467-472.

Martin, J.-L. (2011). Shrimp Aquaculture: From Extensive to Intensive Rearing, the Relationship with the Environment and The Key to Sustainability. In H.-J. Ceccaldi, I. Dekeyser, M. Girault & G. Stora (Eds.), *Global Change: Mankind-Marine Environment Interactions* (pp. 25-30). Dordrecht: Springer.

Martin, M. E., Plourde, L. C., Ollinger, S. V., Smith, M. L., & McNeil, B. E. (2008). A generalizable method for remote sensing of canopy nitrogen across a wide range of forest ecosystems. *Remote Sensing of Environment, 112*(9), 3511-3519.

Meinel, G., & Neubert, M. (2004). *A comparison of segmentation programs for high resolution remote sensing data.* Paper presented at the Geo-Imagery Bridging Continents. XXth ISPRS Congress, Istanbul, Turkey, 12-23 July, 2004.

Mobley, C. D., Sundman, L. K., Davis, C. O., Bowles, J. H., Downes, T. V., Leathers, R. A., et al. (2005). Interpretation of hyperspectral remote-sensing imagery by spectrum matching and look-up tables. *Applied Optics, 44*(17), 3576-3592.

Nagelkerken, I., Blaber, S. J. M., Bouillon, S., Green, P., Haywood, M., Kirton, L. G., et al. (2008). The habitat function of mangroves for terrestrial and marine fauna: A review. *Aquatic Botany, 89*(2), 155-185.

Peterson, D. L., Aber, J. D., Matson, P. A., Card, D. H., Swanberg, N., Wessman, C., et al. (1988). Remote sensing of forest canopy and leaf biochemical contents. *Remote Sensing of Environment, 24*(1), 85-108.

Reef, R., Feller, I. C., & Lovelock, C. E. (2010). Nutrition of mangroves. *Tree Physiology, 30*(9), 1148-1160.

Richardson, A. D., Duigan, S. P., & Berlyn, G. P. (2002). An evaluation of noninvasive methods to estimate foliar chlorophyll content. *New Phytologist, 153*(1), 185-194.

Ruenglertpanyakul, W., Attasat, S., & Wanichpongpan, P. (2004). Nutrient removal from shrimp farm effluent by aquatic plants. *Water Science and Technology, 50*(6), 321-330.

Schlerf, M., Atzberger, C., Hill, J., Buddenbaum, H., Werner, W., & Schüler, G. (2010). Retrieval of chlorophyll and nitrogen in Norway spruce (Picea abies L. Karst.) using imaging spectroscopy. *International Journal of Applied Earth Observation and Geoinformation, 12*(1), 17-26.

Schlerf, M., Verhoef, W., Buddenbaum, H., Hill, J., Atzberger, C., & Skidmore, A. K. (2007). *Comparing three canopy reflectance models with hyperspectral multi-angular satellite data.* Paper presented at the Proceedings of the 10th International Symposium on Physical Measurements and Spectral Signatures in Remote Sensing (ISPMSRS'07), Davos, Switzerland, 12 - 14 March, 2007.

Siciliano, D., Wasson, K., Potts, D. C., & Olsen, R. C. (2008). Evaluating hyperspectral imaging of wetland vegetation as a tool for detecting estuarine nutrient enrichment. *Remote Sensing of Environment, 112*(11), 4020-4033.

Sidik, A. S. (2009). *The changes of mangrove ecosystem in Mahakam delta, Indonesia: A complex social-environmental pattern of linkages in resource utilization.* Paper presented at the The South China Sea Conference 2008. The South China Sea: sustaining ocean productivities, maritime communities and the climate., Kuantan, Malaysia, 25-29 November 2008.

Tilling, A. K., O'Leary, G. J., Ferwerda, J. G., Jones, S. D., Fitzgerald, G. J., Rodriguez, D., et al. (2007). Remote sensing of nitrogen and water stress in wheat. *Field Crops Research*, *104*(1-3), 77-85.

Tomlinson, P. B. (1994). *The Botany of Mangroves*. Cambridge: Cambridge University Press.

Ustin, S. L., Roberts, D. A., Gamon, J. A., Asner, G. P., & Green, R. O. (2004). Using imaging spectroscopy to study ecosystem processes and properties. *Bioscience, 54*(6), 523-534.

Verhoef, W., & Bach, H. (2007). Coupled soil-leaf-canopy and atmosphere radiative transfer modeling to simulate hyperspectral multi-angular surface reflectance and TOA radiance data. *Remote Sensing of Environment, 109*(2), 166-182.

Vohland, M., Mader, S., & Dorigo, W. (2010). Applying different inversion techniques to retrieve stand variables of summer barley with PROSPECT+SAIL. *International Journal of Applied Earth Observation and Geoinformation, 12*(2), 71-80.

Wandera, L. N. N. (2011). *Mapping chlorophyll concentration in a mangrove forest by model inversion approach applied to hyperspectral imagery*. Unpublished MSc. Thesis, University of Twente, Faculty of Geo-Information Science and Earth Observation (ITC).

Zarco-Tejada, P. J., & Sepulcre-Canto, G. (2007). Remote sensing of vegetation biophysical parameters for detecting stress condition and land cover changes. *Estudious de la Zona No Saturada del Sueno*, *8*, 37-44.

Zhang, Y., Chen, J. M., Miller, J. R., & Noland, T. L. (2008). Leaf chlorophyll content retrieval from airborne hyperspectral remote sensing imagery. *Remote Sensing of Environment, 112*(7), 3234-3247.

Appendix

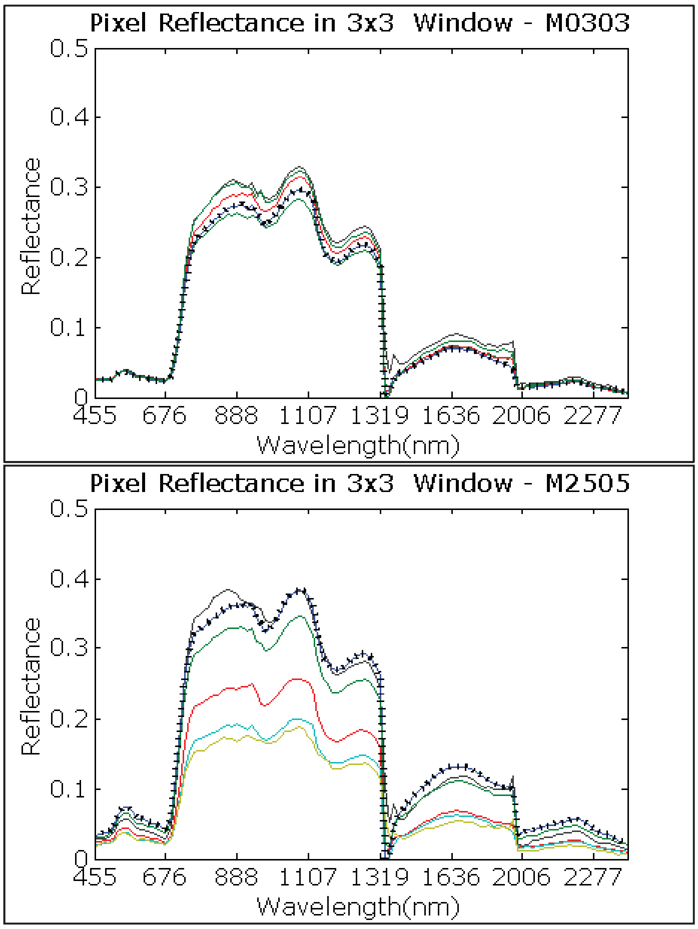

Figure 18: Graphs showing the reflectance per pixel within the window neighbourhood for two sample points: M0303 and M2505. The black dots indicate the pixel in which the field sample was collected. M0303 was accurately predicted and M2505 was poorly predicted.

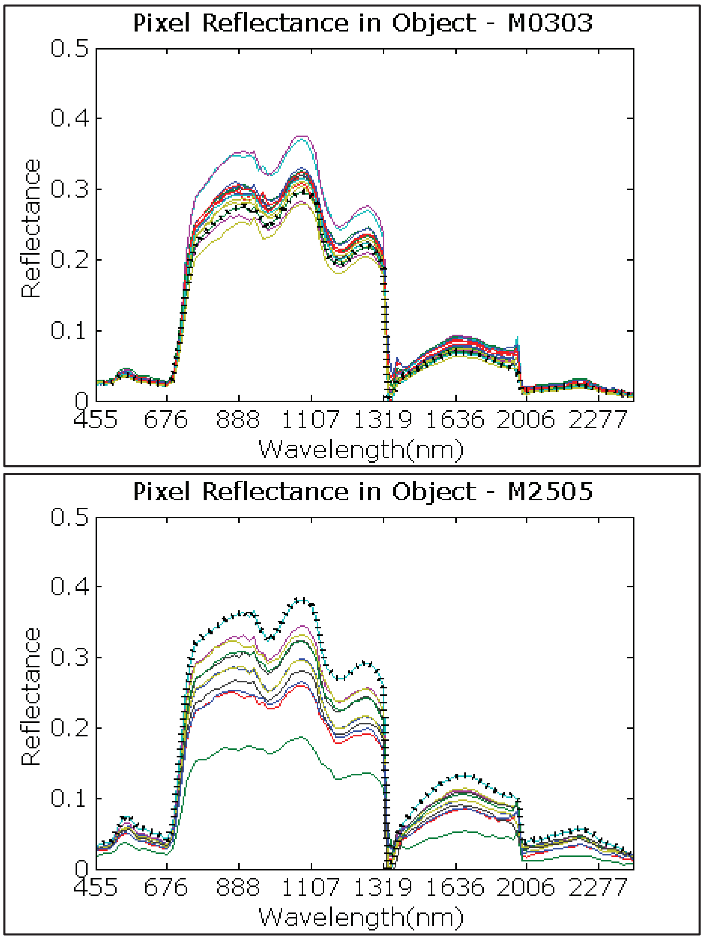

Figure 19: Graph showing the pixel reflectance within object neighbourhoods (scale factor = 2) for two sample points: M0303 and M2505. M0303 was predicted accurately and M2505 was poorly predicted. The pixel which contained the field measurement is shown by black dots.

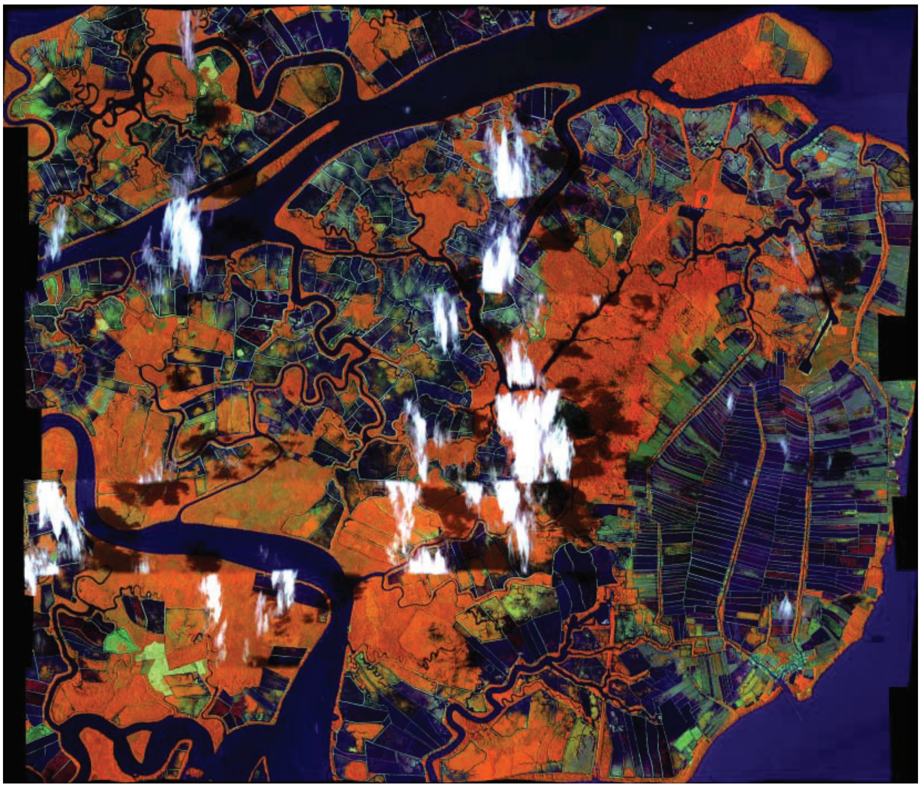

Figure 20: False colour mosaic of the Mahakam delta with only radiometric corrections and georeferencing applied.